Electrophoretic mobility of silica particles in a mixture of toluene and ethanol at different particle concentrations

M. Medrano, A.T. Perez, Laurent Lobry, Francois Peters

Electrophoretic mobility of silica particles in a mixture of

toluene and ethanol at different particle

concentrations

M. Medrano,[†] A. T. Pérez,[*,†] L. Lobry,[‡] and F. Peters[‡]

Departamento de Electrónica y Electromagnetismo, Universidad de Sevilla (Spain), and

Laboratoire de Physique de la Matière Condensé, CNRS-Université de Nice (France)

E-mail: alberto@us.es

Abstract

In this paper we present measurements of the electrophoretic mobility of colloidal particles by using heterodyne detection of light scattering. The measurements have been done up to concentrations of 5.4 % of silica nanoparticles, with a diameter of the order of 80 nm, in a mixture of 70 % toluene and 30 % ethanol. In order to make possible the measurements at these concentrations the liquid mixture is chosen as to match the index of refraction of the particles, thus resulting in a transparent suspension.

[†]Universidad de Sevilla
[‡]Université de Nice

Introduction

Particles of various sorts often acquire charge when are immersed in low conducting liquids. The electric repulsion between the particles contributes to stabilize the suspension. Although this stabilization is in general weaker than for aqueous media, it is of importance in some industrial areas, such as printing and xerography, and from a fundamental point of view.

The charge on the particle surface induces the accumulation of ions of opposite sign around the particle. This gives rise to a structure known as the double layer. When an electric field is applied to a suspension of charged particles, a force appears on both parts of the double layer. This force moves the particles with respect to the liquid with a velocity proportional to the applied field. The coefficient of proportionality is referred to as the electrophoretic mobility. This phenomenon was observed for the first time by Reuss in 1809. Smoluchowski developed the first theory of electrophoresis for one insulated particle when the zeta potential is small and the particle radius is much larger than the Debye length, $\kappa a \gg 1$ (a is the particle radius and κ^{-1} is the Debye length). His well known solution for the electrophoretic mobility is

$$\mu_E = \frac{\varepsilon_r \varepsilon_0 \zeta}{\eta},$$
(1)

where μ_E is the electrophoretic mobility, ε_r is the relative permittivity of the liquid, ε_0 is the dielectric permittivity of the vacuum, ζ is the zeta potential and η is the viscosity of the liquid. On the other hand, Hückel obtained the expression of the mobility for particles with a thick double layer ($\kappa a \ll 1$)

$$\mu_E = \frac{2}{3} \frac{\varepsilon_r \varepsilon_0 \zeta}{\eta}.$$
(2)

Later, Henry joined both electrophoresis relations **within** an analytical expression **that is** valid for a single sphere with small zeta potentials and arbitrary double layer width. He included the function $f(\kappa a)$ in the Smoluchowski expression $\mu_{Henry} = \mu_{Smol} f(\kappa a)$. Function $f(\kappa a)$ is known as the Henry function, this function is 1 when $\kappa a \to \infty$ (Smoluchowski approximation) and it is

2/3 when $\kappa a \to 0$ (Hückel approximation). For thick double layers ($\kappa a < 5$), the Henry function is [1]

$$
\begin{aligned}
f(\kappa a) = \frac{2}{3} + \frac{(\kappa a)^2}{24} - \frac{5(\kappa a)^3}{72} - \frac{(\kappa a)^4}{144} + \frac{(\kappa a)^5}{144} \\
+ \left[\frac{(\kappa a)^4}{12} - \frac{(\kappa a)^6}{144} \right] e^{\kappa a} \int_{\infty}^{\kappa a} \frac{e^{-x}}{x} dx...
\end{aligned}
\tag{3}
$$

Both Smoluchowski and Henry solutions did not include hydrodynamic interactions **between neighboring particles**.

For a finite volume fraction, even without taking into account hydrodynamic interactions or double layer overlap, the electrophoretic mobility depends on the volume fraction for the following **reason: when** the particle moves in one direction, the same volume of liquid **has to move** in the opposite direction. This back flow results in a dependence of the mobility on the particle concentration as [5–8]

$$
\mu_E(\varphi) = \mu_E(0)\left[1 - \varphi\right],
\tag{4}
$$

where φ is the particle solid fraction.

Additionally, when the suspension is composed **of** insulating particles, they alter the distribution of the applied electric field.[8] This fact contributes a $-\varphi/2$ to the expression of μ_E

$$
\mu_E(\varphi) = \mu_E(0)\left[1 - \frac{3}{2}\varphi + O(\varphi^2)\right]
\tag{5}
$$

where $O(\varphi^2)$ denotes terms of order φ^2 and smaller.

Reed and Morrison[3] studied the hydrodynamic interactions for pairs of particles with a thin double layer as function of the interparticle distance. They showed that hydrodynamic and electric interactions cancel each other when the particles have the same zeta potential. In that case, equation (5) is expected to describe the electrophoretic mobility.

However, when the particles have a thick double layer, the interaction between them becomes more complex. As a consequence of the interactions, the electrophoretic mobility decreases as φ

increases more quickly than predicted by equation (5). In this case, the mobility is[4,9]

$$\mu_E(\varphi) = \mu_E(0)\left[1 + S\varphi + O(\varphi^2)\right], \tag{6}$$

where the coefficient S depends on the parameter κa. When κa is smaller than 20, this coefficient decreases quickly. The case of κa as low as 1 has been numerically addressed in Shugai's work.[4] For $\kappa a = 1$, S is much less than -3/2.

For the case of the aqueous media there are some experimental electrophoretic studies, where the effect of the particle concentration on the mobility is measured.[6,10] In our work, we focus on non aqueous systems.

For concentrate suspensions the use of the electrokinetic sonic amplitude (ESA) effect is a suitable technique of measurement.[11] However, ESA works in the MHz range and the results rely on some theoretical assumptions concerning the generation of the sonic wave. Optical techniques are still of application for concentrate suspensions if the liquid is chose as to match the index of refraction of the particles, rendering the suspension transparent.

We study suspensions of silica in a mixture of ethanol and toluene with a technique of photon correlation spectroscopy (PCS). In spite of the fact that there are some commercial apparatuses available, we have used our own system for two reasons. First, we can apply higher electric voltages. Second, we have a better control of the data analysis.

We will first recall the theoretical background concerning the PCS technique. Then we present the materials and the experimental set-up, followed by the experimental results. In the last section, we discuss them in the light of existing theoretical model and numerical computing based on hydrodynamic interactions and double layer overlap.

Theoretical Background

The photon correlation spectroscopy (PCS) is a useful method to characterize colloidal suspensions, micellar systems or biological **materials**. In PCS, a **light** beam is directed **towards** the

sample and the scattered light is detected with an appropriate device, **usually a photomultiplier**.

There are two different PCS methods: homodyne and heterodyne. In the homodyne method only the scattered light impinges on the photocathode. In the heterodyne method, a portion of the unscattered light is mixed with the scattered light on the photomultiplier cathode.

For a set of uncorrelated particles, the autocorrelation function of the light intensity measured by the photomultiplier in heterodyne detection is (see the Appendix for details):

$$C_2(\tau) = 1 + \alpha_2 e^{-\Gamma\tau} \cos(\omega_D \tau). \tag{7}$$

where α_2 is a constant that depends on some experimental parameters, the constant Γ is the product Dq^2, and the Doppler frequency ω_D is defined as

$$\omega_D = \vec{q} \cdot \vec{v} = vq\cos\alpha, \tag{8}$$

where α is the angle between the scattering vector $\vec{q}$ and the particle velocity $\vec{v}$.
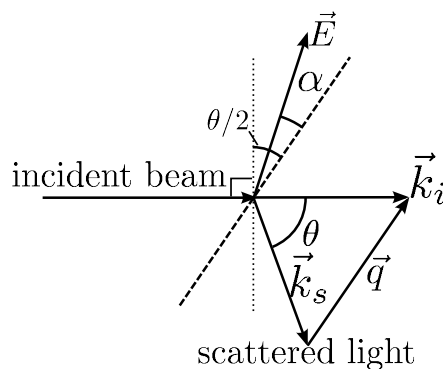

Figure 1: Geometry for an electrophoretic light scattering experiment.

When particle move by electrophoresis their velocity is $\vec{v} = \mu_E \vec{E}$. If the applied electric field is perpendicular to **the** incoming beam, the angle α is $\theta/2$ (see Figure 1). Then the Doppler

frequency is

$$\omega_D = \frac{2\pi n}{\lambda_0} \mu_E E \sin\theta,\tag{9}$$

where E is the module of the electric field and θ is the angle between the incoming and scattered beams. Here, we have supposed that $|\vec{k}_i| \approx |\vec{k}_s|$, then the scattering vector module is $|\vec{q}| = (4\pi n/\lambda_0)\sin(\theta/2)$, where λ_0 is the wave length in the vacuum of the incoming beam, and n is the refraction index of the scattering medium.

In order to obtain Γ and ω_D, we study the real part of the Fourier transform $G_2(\omega)$ of the correlation function $C_2(\tau) - 1$:

$$\mathrm{Re}\,[G_2(\omega)] = \alpha_2 \left(\frac{\Gamma}{\Gamma^2 + (\omega - \omega_D)^2} + \frac{\Gamma}{\Gamma^2 + (\omega + \omega_D)^2} \right).\tag{10}$$

This function is a Lorentzian with the peak placed on ω_D.

If we define the width at mid-height $\omega_{1/2}^{(2)}$ as the frequency at which the value of $\mathrm{Re}[G_2(\omega)]$ is half the maximum value, equation (10) implies that $\omega_{1/2}^{(2)} = \Gamma$.
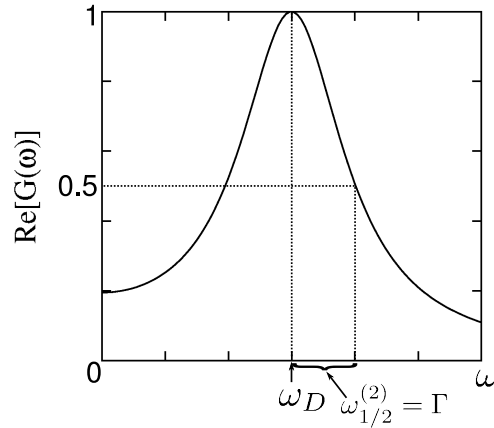

Figure 2: The normalized Fourier transform of the heterodyne correlation function, $C_2(t) - 1$. It shows a peak at the Doppler frequency.

Experiment

Materials

It is often assumed that optical methods are only useful for dilute suspensions, when the sample is transparent. However, it is possible to have a concentrated, yet transparent suspension. The requirement is that the refraction index of the liquid matches that of the particle.[12]

We have synthesized spherical and monodispersed silica nanoparticles by the Stöber method,[13] which consist in hydrolyse tetraethyl-ortosilicate (TEOS) in ethanol, by using ammonia as catalyst. The final product is a suspension of silica particles in a **solution of** ethanol, water, and ammonia. This suspension is called alcosol. The proportion of **reactants that we used** was 0.5 M of TEOS (supplied by Fluka), 0.1 M of distilled water, and 0.2 M of NH_3 **(30 %)** in absolute ethanol. **Ammonia and ethanol were supplied by Panreac.**

For preparing the alcosol, we made two different solutions. The first **contained** 539 ml of ethanol, 22 ml of NH_3, and 31 ml of water. The second **had** 461 ml of ethanol and 130 ml of TEOS. The second solution was added to the first **one** while this was being stirred with a magnetic stirrer. The final mixture was stirred for 3.5 h. The reaction yields 0.31 g of silica **from** 10 ml of alcosol. In a second step, the particle surface was modified with phenyl groups in order to improve the suspension stability and to increase the hydrophobity of the particle surface.[14] Specifically, we added 2.75 ml of phenyltriethoxysilane supplied by Fluka. Under stirring, we left the reaction for one day. The polymer forms a layer on the particle surface providing steric stabilization.

In order to increase the particle concentration, the suspension is centrifuged at 2000 rpm and the supernatant is removed. After each centrifugation, the suspension was redispersed by applying sonication for several minutes. It is important **to prevent the particles from forming** a compact layer at the bottom of the centrifuge tube, because the redispersion **would** be almost impossible to achieve. The next step is to change the remanent liquid by absolute ethanol. **To this end**, we centrifuged the suspension and replaced the supernatant by ethanol. The solid fraction of silica in the absolute ethanol was measured by evaporating a known volume of suspension and by weighing

the dried **residue**. With this procedure the particle concentration obtained was of 18 % in volume, where we have taken a silica density of 2.0 g/cm^3.[15]
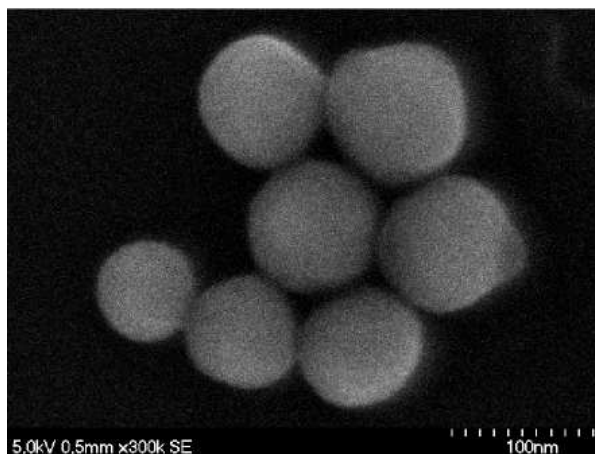

Figure 3: SEM micrograph of the particles.

The particle size was determined by analyzing **a set of** Scanning Electron Microscopy (SEM) photographs. **Figure 3 shows one of this photographs.** The diameter obtained was (88 $\pm$ 8) nm. The **refractive** index of the particles is 1.46 and its density is 2.0 g/cm^3.

The suspension of silica in ethanol is completely opaque. This is due to the difference between the particle and the liquid **refractive indexes**, 1.46 and 1.36 respectively.[15] In order to match the refractive indexes, the suspending liquid was chosen as a mixture of toluene (70 %) and ethanol (30 %).[16] For such a liquid, **we did not observe multiple scattering**, **and the scattered intensity was** sufficiently high for **measurements** to be performed. The conductivity of this mixture was measured to be 6.7 $\pm$ 0.3 μS/m and the relative permittivity was 6.8 $\pm$ 0.5. Both parameters were measured with a device designed and built by the authors.[17,18]

Experimental set-up

Figure 4 shows a diagram of the experimental set-up. The main laser beam is divided into two beams **by means of** a beam splitter. The first beam comes to the measurement cell, **and a lens focusses it at mid-distance between the cell electrodes**. **The second beam** is led directly to the
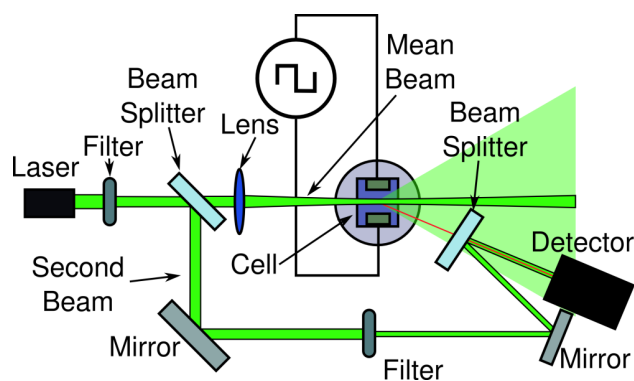
Figure 4: Diagram of the experimental set-up used for the heterodyne detection.

photomultiplier with the help of two mirrors. On the photomultiplier, the second beam and the light scattered by the sample are mixed together. **The electric signal produced by the photomultiplier is sent to** the correlator board **inside** the computer. **The** correlator counts the number of pulses and computes the autocorrelation function.

A set of diaphragms and lens are used to focus the scattered light **onto** the photomultiplier window and to choose the scattering volume of the cell.

The light intensity is regulated with two filters: one is in front of the laser and the other is placed on the **secondary** beam path. These filters allow to choose the intensity ratio between the scattered light and the **secondary** light beam. In heterodyne detection, the intensity of the scattered beam must be at least ten times lower than the **secondary** beam. Thus, the filters have to be changed for each sample, because the scattered light intensity varies **with particle** concentration.

The measurement cell is a dip cell suitable for organic liquids supplied by Malvern. It has a square section of 1 cm **side** and an electrode gap of 2 mm. In order to minimize the refraction of the light, the cell is placed into the center of a cylindrical ethanol bath. The best would have been to use a bath with the same solution toluene-ethanol, but we came up against serious difficulties with the toluene vapor, because it dissolves some plastic pieces that supports the measurement cell. We control the angle of the scattered light with **the help of** goniometer, in our case we use an angle of $25°$. For the calculations it is necessary to correct the scattering angle due to the refraction between the sample ($n = 1.46$) and the ethanol bath ($n = 1.36$). **The** corrected scattering angle is $23.18°$.

We applied for 50 s a symmetric square signal with a frequency of 1 Hz. The temperature

is measured and **monitored** for each measurement, always this has been between 18 and 20 °C.

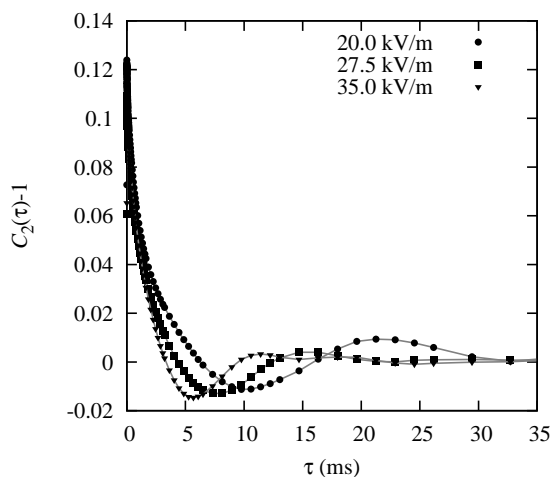# Results and Discussion

Doppler frequency measurement

Figure 5: Example of some heterodyne correlation functions when the particles are undergoing electrophoresis. In this case the suspension has a concentration of particles of 4.5 % in volume. The electrical signal is a symmetric square one with a frequency of 1 Hz and an amplitude of 20.0, 27.5 and 35.0 KV/m.

Figure 5 shows several heterodyne correlation functions computed by the correlator, when the

particles are undergoing electrophoresis. In order to obtain the Doppler frequency from the data set,

we **compute** the Fourier transform of the heterodyne correlation function. **According to equation**

(10), we identify the frequency of the maximum with the Doppler frequency. Figure 6 shows

the spectrum of the correlation function for a voltage of 50 V between the electrodes (25 KV/m).

Mobility measurement

In order to determine the electrophoretic mobility, we measure the Doppler frequency for several

electric fields. Figure 7 plots the Doppler frequencies versus the applied electric field for a suspen-
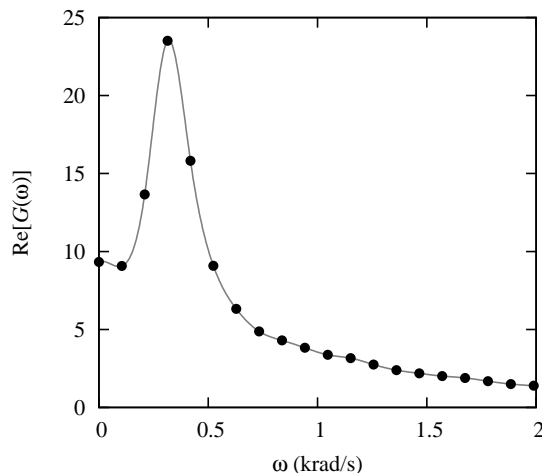
Figure 6: The function $G(\omega)$ is the Fourier transform of $C_2(\tau) - 1$. This figure corresponds to the data obtained for an applied electric field of 25 KV/m to our suspension. The particle concentration is 4.5 % in volume. It shows a peak at the Doppler frequency.

sion with a particle concentration 4.5 % in volume. The **frequency** values have a linear relation with the applied voltage, **as relation (9) predicts**. The electrophoretic mobility is obtained from the slope of this straight line.

By using this method, we have obtained the electrophoretic mobility for several particle concentrations. Specifically, the particle concentrations was **varied** from 0.32 % to 5.4 % in volume.

The values of the mobility measurements with their error bars, are shown **in** Figure 8. For certain values of the electric field, we have also measured the mobility of the samples using a nano zetasizer of Malvern. The results are compatible with values obtained by PCS method. The zetasizer allows to determine the sign of the particle charge, which is negative.

Figure 8 shows how the electrophoretic mobility decreases with the particle concentration. Since we worked with semi-dilute suspensions ($\varphi < 0.06$), the values of the electrophoretic mobility can be fitted to relation (6) discarding the term $O(\varphi^2)$:

$$|\mu_E(0)| = (2.7 \pm 0.2)\, 10^{-9}\, \text{m}^2/\text{Vs}$$

$$S = -8 \pm 2$$

This shows that μ_E decreases with particle concentration faster than predicted by relation (5),

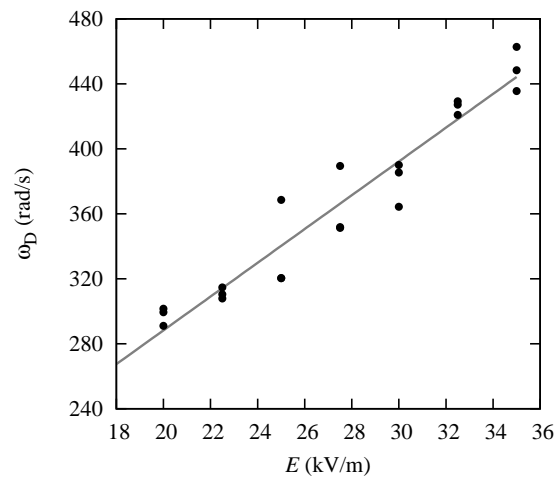11

Figure 7: Doppler frequency versus applied electric field between the electrodes. The particle concentration is 4.5 % in volume. The straight line is the **least square fit** to the data. We have taken several measurements of ω_D for each value of the electric field.
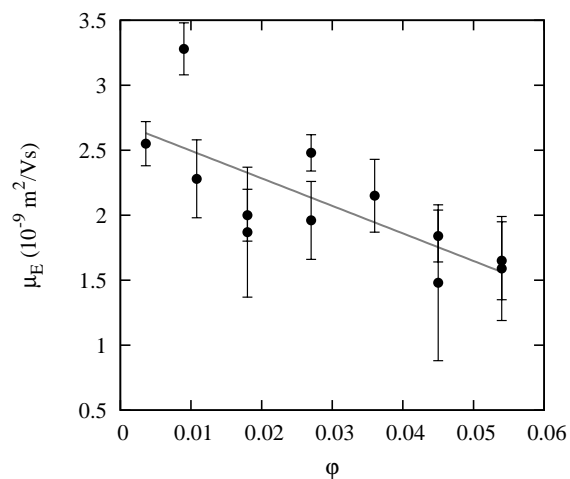

Figure 8: Electrophoretic mobility versus solid fraction. Each point in the plot corresponds to a different sample.

which corresponds to $\kappa a \gg 1$.

Mobility polydispersity

When the applied electric field increases the Doppler frequency also increases. At first sight, and since the factor $e^{-\Gamma\tau}$ in equation (27) does not depend on the electric field, the heterodyne autocorrelation function **should** have more **visible** oscillations as the electric field increases. Therefore, for higher electric field, we expect that the spectrum peaks will lie farther from the origin **and be** better resolved. But Figure 5 shows that the number of visible oscillations in the correlation function does not increase with the electric field. In fact this figure shows that the amplitude of the correlation function decreases faster for larger fields. Moreover, what it is observed experimentally is a broadening of the peaks in the Fourier transform of the correlation function as the electric field **increases (see Figure 9)**. Besides, a decrease in the value of the maximum **value** is found.
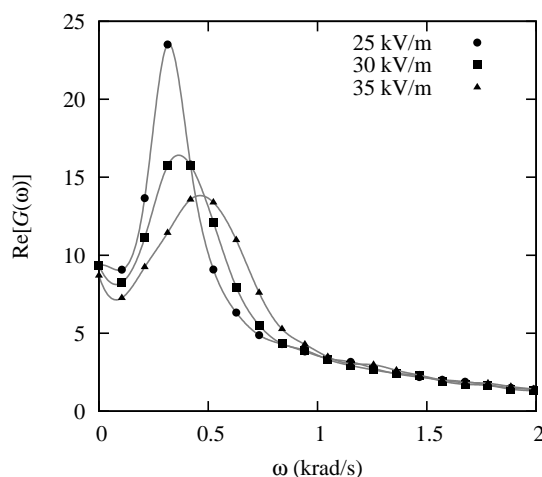

Figure 9: Fourier transform of the heterodyne correlation function for three values of the electric field. The Doppler frequency **increases** with the electric field, **and** the peaks become smaller and wider.

This effect was noticed in other works,[10,20] where it is attributed to a diffusion coefficient dependence on the electric field. Effectively, accordingly to equation (10), the coefficient Γ increases apparently with the applied voltages. Furthermore, the equation (10) implies that the broadening of the peaks is due to increase of Γ. However, this **is** not physically sound, since the diffusion

coefficient is directly related to the particle size.

On the other hand, Wu[21] suggests that a broadening of the peaks in heterodyne spectra is due to a mobility polydispersity. In fact, the expression (26) is valid only if the particles have all the same electrophoretic velocity. But, if there is a electrophoretic velocity distribution or, in other words, a Doppler frequency distribution, the effect of this polydispersity **will affect the correlation functions**.

To analyze the effect let us assume a Gaussian distribution of Doppler frequencies

$$P(\omega_D) = \frac{1}{\sqrt{2\pi}\sigma_\omega} e^{-\frac{(\omega_D - \omega_{D0})^2}{2\sigma_\omega^2}}, \tag{11}$$

where ω_{D0} is the average Doppler frequency and σ_ω is its dispersion. The new correlation function of the electric field is

$$g(t) = \int_{-\infty}^{+\infty} \frac{1}{\sqrt{2\pi}\sigma_\omega} e^{-\frac{(\omega_D - \omega_{D0})^2}{2\sigma_\omega^2}} e^{(-\Gamma + i\omega_D)t} d\omega_D$$
$$= e^{-\Gamma t} e^{-\sigma_\omega^2 t^2} e^{i\omega_{D0}t}. \tag{12}$$

With this new expression of the correlation function of the light electric field **and equation** (23), **the expression of the correlation function for heterodyne detection is**

$$C_2(t) = 1 + \alpha_2 \text{Re}[g(t)] = 1 + \alpha_2 e^{-\Gamma t - \sigma_\omega^2 t^2} \cos(\omega_{D0}t). \tag{13}$$

This expression shows that the relaxation time of the correlation functions depends on the Doppler frequency dispersion.

The Fourier transform of correlation function (13) has not an analytical expression. But we can calculate the limits when $\sigma_\omega \ll \Gamma$ and $\sigma_\omega \gg \Gamma$. For the first case, we can take $\sigma_\omega \to 0$, then the Fourier transform will be relation (10). In the second case, where the frequency dispersion

dominates, we can take the limit $\Gamma \to 0$, then the Fourier transform of equation (13) is

$$\mathrm{Re}[G_2(\omega)] = \frac{1}{2}\frac{\sqrt{2\pi}}{\sigma_\omega}\left[\exp\left(-\frac{(\omega - \omega_{D0})^2}{2\sigma_\omega^2}\right) + \right.$$
$$\left. \exp\left(-\frac{(\omega + \omega_{D0})^2}{2\sigma_\omega^2}\right)\right]. \tag{14}$$

For high electric fields, where we can neglect the diffusion term in the autocorrelation functions, **the frequency** $\omega_{1/2}^{(2)}$ **is determined** by the frequency dispersion

$$\omega_{1/2}^{(2)} = \sigma_\omega\sqrt{2\ln 2}. \tag{15}$$

The interesting point is that σ_ω depends on the electric field, since

$$\omega_D = \frac{2\pi n}{\lambda}\sin(\theta)\mu_E E$$
$$\sigma_\omega = \frac{2\pi n}{\lambda}\sin(\theta)\sigma_\mu E, \tag{16}$$

where μ_E is the electrophoretic mobility and σ_μ is its dispersion. Therefore, $\omega_{1/2}^{(2)}$ **increases** linearly with E.

Relation (16) explains the peak broadening in the heterodyne autocorrelation function (see Figure 9). In short, for small electric fields, the relaxation time of the correlation functions is dominated by the diffusion coefficient, whereas for high electric fields the frequency dispersion dominates. Another important conclusion is that mobility polydispersity only affects the width of the peaks, whereas the average Doppler frequency does not vary.

On the other hand, due to mobility polydispersity the autocorrelation function decays in a time of order σ_ω^{-1}. The period of the oscillations of the same function is ω_D^{-1}. Both quantities depend on the electric field, as equation (16) shows, but their ratio is independent of it. **However**, we can

not measure σ_ω directly, **but only** the value of $\omega_{1/2}^{(2)}$. In fact

$$\frac{1/\omega_{1/2}^{(2)}}{1/\omega_D} = \frac{\mu_E}{\sigma_\mu \sqrt{2\ln 2}}, \tag{17}$$

that can be used to calculate the value of σ_μ.

Although we have assumed a Gaussian distribution of Doppler frequencies, this will not be so in general. However, the main conclusion that the **value $\omega_{1/2}^{(2)}$ increases** with the electric field due to the mobility polydispersity, will remain true. Even more, equation

(17) can be used, at least, as an estimation of the mobility polydispersity σ_μ.

Table 1:   Ratio between the Doppler frequency, ω_D, and $\omega_{1/2}^{(2)}$. It tends to a constant value close to 0.6. The concentration of particles is 4.5 % in volume.

E (KV/m)	ω_D (rad/s)	$\omega_{1/2}^{(2)}$ (rad/s)	$\frac{\omega_{1/2}^{(2)}}{\omega_D}$
25.0	320	63	0.20
27.5	352	214	0.61
30.0	364	238	0.66
32.5	434	251	0.58
35.0	439	283	0.64

Table Table 1 shows how the ratio between **the** Doppler frequency **and** $\omega_{1/2}^{(2)}$ does not change with the electric field when this is high enough. From the data of table Table 1, we can estimate experimentally the mobility dispersion σ_μ if we take $\omega_{1/2}^{(2)}/\omega_D \approx \sigma_\mu/\mu_E$. **The** mobility dispersion results **of the order of** $0.6\mu_E$.

Discussion

First, it is worth evaluating the double layer thickness. We did not add electrolyte to the suspension, therefore, the double layer is formed from solvent molecules and impurities. In order to estimate

the Debye length, we use the expression:

$$\kappa^{-1} = \sqrt{\frac{D\varepsilon_r\varepsilon_0}{\sigma}}, \tag{18}$$

where ε_0 is the dielectric permittivity of the **vacuum,** ε_r is the relative permittivity of the toluene-ethanol mixture, D **is the diffusion coefficient of ions and** σ **the electrical conductivity of the liquid.**

Considering a typical value for the diffusion coefficient of order of 10^{-9} m^2/s and **the measured value for the conductivity**, we obtain $\kappa^{-1} \approx 90$ nm and $\kappa a \approx 0.44$. Under these conditions particle-particle forces cannot be neglected. In fact, the typical distance between particles varies from 500 nm, for a concentration of 0.36 %, to less than 200 nm for concentrations higher than 4.5 %; this leads to overlap of the double layers.

In Shugai's work,[4] the mobility of suspensions with thick double layer is numerically studied. In addition to κ^{-1}, another characteristic length enters the pair correlations functions $g(r)$. **This** is the Bjerrum length

$$\lambda_B = \frac{e^2}{4\pi\varepsilon_0\varepsilon_r k_B T}. \tag{19}$$

In our case, $a\lambda_B^{-1} \approx 5$. **Shugai** *et al,*[4] **for** $\kappa a = 1$ **and** $a\lambda_B^{-1} = 10$**, obtained for the parameter of** equation (6) $S \approx -6$. The experimental measurement that we have performed is thus in quite good agreement with this numerical result.

Another important point discussed by Ennis[9] and Shugai[4] is the following: due to hydrodynamic interactions between pair of particles, the mobility in a direction parallel to the line of **their** centers is different from the mobility in the transverse direction. As a consequence, in suspension, the particle velocity has fluctuating components, leading to mobility dispersion. For $a\lambda_B^{-1} = 10$ and $\kappa a = 1$, Shungai *et al* computes the fluctuation in particle mobility $\frac{\sigma_\mu}{\mu_E} \approx 7 \cdot 10^{-2}$.

For smaller values of $a\lambda_B^{-1}$ and κa, Shugai *et al* show that a larger value of $\sigma_\mu\mu_E^{-1}$ is expected. **Therefore, our** measurements are in qualitative agreement with the numerical computation.

Other sources of mobility dispersion should be taken in account. First, the 10 % size poly-

dispersity could have implications in the mobility dispersion. Unfortunately, this has not been numerically explored in the work by Shugai *et al*. Another factor is the surface charge polydispersity. When $\varphi \to 0$, the electrophoretic mobility must agree with Henry equation. In our case, where $\kappa a \approx 0.44$, Hückel equation (2) is precise enough to give the zeta potential from the mobility at $\varphi = 0$:

$$\zeta = (47 \pm 3)\text{mV}.$$

Assuming that the zeta potential is the potential at the particle surface, the total charge over each particle can be estimated from the expression

$$Q = 4\pi\varepsilon_0\varepsilon_r a\zeta. \tag{20}$$

We estimate **that** the number of elementary charges **is approximately 10.** This small quantity implies that any variation of the electrical charge produces large dispersion of the zeta potential, and, hence, of the mobility.

Conclusion

In conclusion, the technique of index of refraction matching has allowed us to study the electrophoretic mobility of concentrated suspension by PCS. It has been found that the mobility of the particles decreases with the concentration faster than $1 - 1.5\varphi$, which indicates that the interactions between the particles are important. **The** measured mean mobility is in good agreement with the numerical computing by Shugai *et al*. This experimental technique enabled us to measure the mobility polydispersity as well. This polydispersity has been seldom measured in the past. We think that this is a useful method to get insight in the velocity fluctuations in electrophoresis.

Acknowledgement

References

(1) D. C. Henry, *Proc. R. Soc. London Ser. A* **1931**, *133*, 106.

(2) R. W. O'Brien and L. R. White, *J. Chem. Soc. Faraday Trans. II* **1978**, *74*, 1607.

(3) L. D. Reed and F. A. Morrison, *J. Colloid Interface Sci.* **1975**, *54*, 117.

(4) Alexander A. Shugai, Steven L. Carnie, Derek Y. C. Chan and John L. Anderson, *J. Colloid Interface Sci.* **1997**, *191*, 357.

(5) J. L. Anderson, *J. Colloid Interface Sci.* **1981**, *82*, 248.

(6) C. F. Zukoski IV and D. A. Saville, *J. Colloid Interface Sci.* **1987**, *115*, 422.

(7) A. T. Pérez and E. Lemaire, *J. Colloid Interface Sci.* **2004**, *279*, 259.

(8) S. Ahualli, A. V. Delgado and C. Grosse, *J. Colloid Interface Sci.* **2006**, *301*, 660.

(9) J. Ennis and L. R. White, *J. Colloid Interface Sci.* **1996**, *185*, 157.

(10) H. Reiber, T. Köller, T. Palberg, F. Carrique, E. Ruiz-Reina and R. Piazza, *J. Colloid Interface Sci.* **2007**, *309*, 315.

(11) R. J. Hunter, *Colloids Surfaces A: Physicochem. Eng. Aspects* **1998**, *141*, 37.

(12) J. K. Phalakornkul, A. P. Gast and R. Pecora, *Phys. Rev. E* **1996**, *54*, 661.

(13) W. Stöber and A. Fink, *J. Colloid Interface Sci.* **1968**, *26*, 62.

(14) Z. Wu, H. Xiang, T. Kim, M. S. Chun and K. Lee, *J. Colloid Interface Sci.* **2006**, *304*, 119.

(15) C. W. Robert *Handbook of Chemistry and Physics* CRC Press, Inc.: Ohio (1974).

(16) A. P. Philipse and A. Vrij, *J. Colloid Interface Sci.* **1989**, *128*, 121.

(17) M. Medrano, A. T. Pérez and C. Soria-Hoyo, *J. Phys. D: Appl.* **2007**, *40*, 1477.

(18) M. Medrano, A. T. Pérez and C. Soria-Hoyo, *IEEE Transactions on Dielectrics and Electrical Insulation*, In press.

(19) Berne B and Pecora R 1976 *Dynamic Light Scattering* J. Willey ed. (1976).

(20) T. Palberg and H. Versmold, *J. Phys Chem.* **1989**, *93*, 5296.

(21) Xu R, *Langmuir* **1993**, *9*, 2955.

Appendix

The autocorrelation function is defined as

$$C(\tau) = \frac{\langle I(t)I(t+\tau)\rangle}{\langle I(t)\rangle^2},$$

(21)

where $I(t)$ is the light intensity at the initial time t and τ is the time lag. The symbols $\langle\rangle$ denote temporal average.

The correlation function (21) may be expressed in terms of the correlation function of the electric field of the scattered light $g(\tau)$.

For homodyne detection, the correlation function is [19]

$$C_1(\tau) = 1 + \alpha_1|g(\tau)|^2$$

(22)

and for heterodyne detection

$$C_2(\tau) = 1 + \alpha_2 \text{Re}[g(\tau)] \tag{23}$$

where α_1 and α_2 are constants depending on experimental parameters, such as the coherence area, and the ratio between the scattered light and the direct beam intensity, for the heterodyne case. The symbol Re denotes the real part of the complex function $g(\tau)$.

The correlation function of the electric field of the scattered light is

$$g(\tau) = \frac{\langle \vec{E}(t) \cdot \vec{E}^*(t+\tau) \rangle}{\langle \vec{E}(t) \cdot \vec{E}^*(t) \rangle} \tag{24}$$

where $\vec{E}$ is the electric field of the light scattered by the scattering volume and $\vec{E}^*$ denotes its complex conjugate.

For uncorrelated particles, the equation (24) becomes[19]

$$g(\vec{q}, \tau) = e^{-\Gamma \tau} e^{i \omega_D \tau}, \tag{25}$$

where Γ is the product Dq^2, $\vec{q}$ the scattering vector ($\vec{q} = \vec{k}_i - \vec{k}_s$), D the diffusion coefficient and ω_D is the Doppler frequency.

Using equation (25), the correlation functions (22) and (23) take the form

$$C_1(\tau) = 1 + \alpha_1 e^{-2\Gamma \tau} \tag{26}$$

and

$$C_2(\tau) = 1 + \alpha_2 e^{-\Gamma \tau} \cos(\omega_D \tau). \tag{27}$$